

Semi-Centralised Multi-Agent Reinforcement Learning with Policy-Embedded Training

Taher Jafferjee^{1,*}, Juliusz Ziomek^{1,*}, Tianpei Yang², Zipeng Dai¹,
 Jianhong Wang³, Matthew Taylor², Kun Shao¹, Jun Wang⁴, David Mguni^{†1}

¹Huawei Noah’s Ark Lab ²University of Alberta
³Imperial College, London ⁴University College, London

Abstract

Centralised training (CT) is the basis for many popular multi-agent reinforcement learning (MARL) methods because it allows agents to quickly learn high-performing policies. However, CT relies on agents learning from one-off observations of other agents’ actions at a given state. Because MARL agents explore and update their policies during training, these observations often provide poor predictions about other agents’ behaviour and the expected return for a given action. CT methods therefore suffer from high variance and error-prone estimates, harming learning. CT methods also suffer from explosive growth in complexity due to the reliance on global observations, unless strong factorisation restrictions are imposed (e.g., monotonic reward functions for QMIX). We address these challenges with a new *semi-centralised* MARL framework that performs *policy-embedded* training and decentralised execution. Our method, policy embedded reinforcement learning algorithm (PERLA), is an enhancement tool for Actor-Critic MARL algorithms that leverages a novel parameter sharing protocol and policy embedding method to maintain estimates that account for other agents’ behaviour. Our theory proves PERLA dramatically reduces the variance in value estimates. Unlike various CT methods, PERLA, which seamlessly adopts MARL algorithms, scales easily with the number of agents without the need for restrictive factorisation assumptions. We demonstrate PERLA’s superior empirical performance and efficient scaling in benchmark environments including *StarCraft Micromanagement II* and *Multi-agent Mujoco*.

1 Introduction

Multi-agent reinforcement learning (MARL) has emerged as a powerful tool to enable autonomous agents to tackle difficult tasks such as ride-sharing (Zhou et al. 2020) and swarm robotics (Mguni, Jennings, and de Cote 2018). Recently, various methodologies have produced significant performance boosts for MARL algorithms (Mguni et al. 2021b; Kuba et al. 2021). Nevertheless, an important impediment for MARL is the high variance of the critic and policy gradient estimators. Reducing this variance is a critical challenge since high variance estimates can significantly hinder training, leading to low sample efficiency and poor overall performance (Gu et al. 2016). This variance has multiple

causes. First, MARL methods are applied to unknown environments whose reward signals are often noisy, especially as the sizes of the state and action spaces increases (Kuba et al. 2021). Second, unlike in single agent reinforcement learning (RL), MARL agents are faced with the challenge of distinguishing the aleatoric uncertainty due to environmental stochasticity from randomness due to agents’ exploratory actions. These challenges can deeply undermine the performance of MARL methods, especially in centralised learning (CL) methods where agents rely on observations of others’ actions while training.

CL serves as the foundation for many popular MARL methods such as MAPPO (Yu et al. 2021a), Q-DPP (Yang et al. 2020) QMIX (Rashid et al. 2018), SPOT-AC (Mguni et al. 2021a), and COMA (Foerster et al. 2018b). In CL, each agent has a (possibly shared) critic that makes use of all available information generated by the system, including the global state and the joint action (Peng et al. 2017). Accounting for actions of other agents is crucial to achieve good coordination. Despite the obvious advantages from using knowledge of the joint actions in the critic, this methodology has several weaknesses that exacerbate the MARL variance problem. The Q-functions are based on *one-off* observations of actions sampled from other agents’ policies at a given state. This can produce VF updates based on improbable events and hence, inaccurate estimates of expected returns, leading to higher variance value function (VF) estimates. Also, since each agent’s critic has an explicit dependence on the actions of others, the CL critic suffers from an explosive growth in complexity with the number of agents (Yang and Wang 2020). This results in CL methods needing large numbers of samples to complete training. Current methods for alleviating this rely on VF factorisations that require restrictive representational constraints. These constraints can cause poor exploration and performance failures when violated (Mahajan et al. 2019) (e.g., QMIX (Rashid et al. 2018) requires a monotonicity constraint that can produce suboptimal value approximation).

Because of these issues affecting CL, (decentralised) independent learning (IL) represents an attractive alternative (de Witt et al. 2020a). IL decomposes a MARL problem with N agents into N decentralised single-agent problems while the agents train solely with local observations. This avoids the explosive growth in complexity suffered by CL methods.

* Equal Contribution.

† Corresponding author: davidmguni@hotmail.com.

Nonetheless, since MARL environments consist of multiple learners, IL suffer from convergence issues (Yang and Wang 2020). Additionally, since IL methods cannot explicitly factor in the behaviour of other agents, achieving coordination among IL agents can be a difficult to achieve, resulting in suboptimal performance in some tasks.

To tackle these challenges, in this paper we propose a new MARL training formalism which we call *semi-centralised* training. In this framework, the agents use knowledge of other agents' policies to compute accurate VFs estimates while using a critic (and policy) that has only the agent's own action and state as an input. Specifically, we introduce *policy embedding*, a technique that enables the agents' VF estimates to capture the present and future behaviour of other agents. As with parameter sharing, a technique used in many MARL methods (e.g., MAPPO (Yu et al. 2021a), QMIX (Rashid et al. 2018)), this procedure requires the agents to communicate their individual policies during training.

Our framework, policy embedding reinforcement learning algorithm (PERLA), embeds the agents' policies within the critic estimation. This is done by sampling the actions of other agents and using them to marginalise the influence of other agents from the critic. The method is scalable and the resulting critic retains a functional form that requires only the agent's own action (and state) as input to the action-value function. Consequently, the resulting critic exhibits the efficient scaling benefits of a fully decentralised critic while **preserving the convergence guarantees** and coordination abilities of a centralised critic.

Many leading MARL methods such as MAPPO (Yu et al. 2021a), IPPO (de Witt et al. 2020a), MADDPG (Lowe et al. 2017) use the actor-critic formalism. For concreteness, we instantiate our methodology within actor-critic architectures which involve both critic and policy updates which is a natural candidate to instantiate our framework. We propose Algorithm 1, which is a PERLA version of MAPPO/IPPO and show it improves the performance of the underlying algorithm. Applications of PERLA could naturally be extended to other degenerate architectures (e.g. value-based methods).

We summarise the advantages of PERLA below.

1) PERLA enables (networked) MARL agents to scale efficiently by factoring the joint policy into a new functional representation of the critic. Crucially, each agent's critic does not use a joint action input. This enables efficient scaling with the number of agents without restrictive VF constraints (validated empirically in Sec. 5.2).

2) Elimination of non-stationarity of IL by incorporating updated policies into the agents' critics through the policy embedding procedure. This avoids the non-stationarity problem in MARL when critics use localised observations.

3) Plug & play enhancement because PERLA can seamlessly incorporate different Actor-Critic algorithms, PERLA significantly boosts performance over the base MARL learners PPO (Schulman et al. 2017), and MAPPO (Yu et al. 2021a) (validated empirically Sec. 5.1).

4) PERLA is theoretically sound and we prove that

i) PERLA induces a vast reduction of variance of VF estimates (Theorem 1), *ii*) PERLA preserves policy gradient estimators (Theorem 3), and *iii*) Actor-Critic style algorithm

based on PERLA converges almost surely to a locally optimal policy profile (Theorem 6).

2 Related Work

Centralised Learning CL is assured to generate policies that are consistent with the desired system goal whenever the IGM principle (Son et al. 2019) is satisfied.¹ In order to realise the IGM principle in the CL framework, QMIX and VDN propose two sufficient conditions of IGM to factorise the joint action-value function. Such decompositions are limited by the joint action-value function class they can represent and can perform badly in systems that do not adhere to these conditions (Wang et al. 2020). QPLEX (Wang et al. 2020) uses a dueling network architecture to factor the joint action-value function. It however has been shown to fail in simple tasks with non-monotonic VFs (Rashid et al. 2020). QTRAN (Son et al. 2019) formulates the MARL problem as a constrained optimisation problem but has been shown to scale poorly in complex MARL tasks such as the StarCraft Multi-Agent Challenge (SMAC) (Peng et al. 2020). WQMIX (Rashid et al. 2020) considers a weighted projection towards better performing joint actions but does not guarantee IGM consistency. Actor-critic methods such as COMA (Foerster et al. 2018b) and MADDPG (Lowe et al. 2017) are popular methods within MARL. Although these methods use CL without restrictive assumptions, they are significantly outperformed by value-based methods such as QMIX and MAPPO (Yu et al. 2021a) on standard MARL benchmarks like SMAC (Peng et al. 2020). Consequently, achieving full expressiveness of the IGM function class with scalability remains an open challenge for MARL.

Parameter Sharing (PS) (Gupta, Egorov, and Kochenderfer 2017) aims to speed up learning by sharing the policy parameters of all the agents during training. In this setup, all agents share the same policy network forcing the agents to share the same policy which is only appropriate in systems with rich symmetries between agents. Leading MARL methods such as MAPPO use PS with proven performance benefits in benchmark domains. Our goal differs from PS since the benefit of PERLA is to enable the agents to embed knowledge of the other agents' behaviours into the agent's own critic estimation and policy. As in PS, PERLA requires communication between agents during training, but in PERLA each agent can maintain its own set of parameters, which is more suitable for environments where agents significantly differ from each other.

Opponent Modelling allows each agent to infer the other agents' policies from their observed behavior. This is widely used in MARL with imperfect information. LOLA (Foerster et al. 2018a) and its recent variant of COLA (Willi et al. 2022) seeks to model the impact of an agent's policy on the opponent's future policy updates. Through behavioral cloning, the agent infers the opponent's parameters from the corresponding state-action trajectories. Based on unsupervised representation learning, several methods predict the other agents' actions by using each agents' own policy ar-

¹The IGM principle imposes an equivalence between the joint greedy action and the collection of individual greedy actions.

chitecture (Raileanu et al. 2018) or auxiliary policy features (Grover et al. 2018; Hong et al. 2018). MBOM (Yu et al. 2021b) uses the (provided) environment model to simulate multiple best response policies as opponents and then mixes them according to the similarity with the real behaviors of opponents. However, MBOM were examined only in two-player games. In contrast with this set of methods that introduce prediction models to (over)fit an opponent’s trajectories, in PERLA agents communicate their policy parameters (and local observations) to each other during training. With this and using our novel *policy embedding procedure* allows the agents to immediately form best responses to the joint policies of other agents.

3 PERLA framework

We formulate the MARL problem as a Markov game (MG) (Deng et al. 2021), which is represented by a tuple $\mathcal{G} = \langle \mathcal{N}, \mathcal{S}, (\mathcal{A}_i)_{i \in \mathcal{N}}, P, R_i, \gamma \rangle$ where \mathcal{S} is the finite set of states, \mathcal{A}_i is an action set for agent $i \in \mathcal{N}$, and $R_i : \mathcal{S} \times \mathcal{A} \rightarrow \mathcal{P}(D)$ is the reward function that agent i seeks to maximise (where D is a compact subset of \mathbb{R}), and $P : \mathcal{S} \times \mathcal{A} \times \mathcal{S} \rightarrow [0, 1]$ is the probability function describing the system dynamics where $\mathcal{A} := \times_{i=1}^N \mathcal{A}_i$. We consider a partially observable setting, in which given the system state $s^t \in \mathcal{S}$, each agent $i \in \mathcal{N}$ makes local observations $\tau_i^t = O(s^t, i)$ where $O : \mathcal{S} \times \mathcal{N} \rightarrow \mathcal{Z}_i$ is the observation function and \mathcal{Z}_i is the set of local observations for agent i . To decide its actions, each agent $i \in \mathcal{N}$ samples its actions from a *Markov policy* $\pi_{i, \theta_i} : \mathcal{Z}_i \times \mathcal{A}_i \rightarrow [0, 1]$, which is parameterised by the vector $\theta_i \in \mathbb{R}^d$. Throughout the paper, π_{i, θ_i} is abbreviated as π_i . At each time $t \in 0, 1, \dots$, the system is in state $s^t \in \mathcal{S}$ and each agent $i \in \mathcal{N}$ takes an action $a_i^t \in \mathcal{A}_i$, which together with the actions of other agents $\mathbf{a}_{-i}^t := (a_1^t, \dots, a_{i-1}^t, a_{i+1}^t, \dots, a_N^t)$, produces an immediate reward $r_i \sim R(s^t, \mathbf{a}_i^t)$ for agent $i \in \mathcal{N}$. The system then transitions to a next state $s^{t+1} \in \mathcal{S}$ with probability $P(s^{t+1} | s^t, \mathbf{a}^t)$ where $\mathbf{a}^t = (a_1^t, \dots, a_N^t) \in \mathcal{A}$ is the *joint action* which is sampled from the *joint policy* $\pi := \prod_{i=1}^N \pi_i$. The goal of each agent i is to maximise its expected returns measured by its VF $v_i(s) = \mathbb{E}[\sum_{t=0}^{\infty} \gamma^t R_i(s^t, \mathbf{a}^t) | s_0 = s]$ and the action-value function for each agent $i \in \mathcal{N}$ is given by $Q_i(s, \mathbf{a}) = \mathbb{E}[\sum_{t=0}^{\infty} R_i(s^t, \mathbf{a}^t) | \mathbf{a}^0 = \mathbf{a}]$, where $-i$ denotes the tuple of agents excluding agent i . Likewise, we denote $\prod_{j=1, j \neq i}^N \pi_j$ as π_{-i} . In the fully cooperative case all agents share the same goal: $R_1 = \dots = R_N := R$.

In the CL paradigm, given a state $s \in \mathcal{S}$ and the joint action $\mathbf{a} \in \mathcal{A}$, each agent $i \in \mathcal{N}$ computes its action-value function $Q_i(s, \mathbf{a})$. The action-value function provides an estimate of the agent’s expected return using its policy given the behaviour of all other agents $\mathcal{N}/\{i\}$ for a given action $a_i \in \mathcal{A}_i$. Therefore, $Q_i(s, \mathbf{a})$ seeks to provide an estimate of the agent’s own action, accounting for the actions of others. MARL agents use stochastic policies to explore — each joint action $\mathbf{a} \sim \pi$ may contain exploratory actions that included in agent policy updates.

The core component of the PERLA framework is a Critic Policy Embedding procedure. As the name suggests, the procedure embeds the agents’ policies within the critic, en-

abling us to construct a critic whose input takes only the agent’s own action and the state while factoring in the joint behaviour of other agents. This is done by jointly marginalising the action-value function \tilde{Q}_i , as defined below:

$$\tilde{Q}_i(s, a_i) := \mathbb{E}_{\pi_{-i}} [Q_i(s, \mathbf{a})]; \quad \mathbf{a} \equiv (a_i, \mathbf{a}_{-i}) \in \mathcal{A}, \quad (1)$$

where $s \in \mathcal{S}$, $a_i \sim \pi_i(\cdot | \tau_i)$, $\mathbf{a}_{-i} \sim \pi_{-i}(\cdot | \tau_{-i})$. This object requires some explanation: as with Q_i , the function \tilde{Q}_i seeks to estimate the expected return following agent i taking action a_i . However, unlike Q_i , \tilde{Q}_i builds in the distribution of the actions played by other agents *under their current policy*. This gives less weight to low probability actions and conversely for high probability actions. A key aspect is that \tilde{Q} depends only on the agent’s own action (and state) which acquires the scalability benefit of IL while factoring in the behaviour of other agents. As in practice, it may be impossible to analytically calculate 1, to approximate $\tilde{Q}_i(s, a_i)$, for any $s \in \mathcal{S}$ and any $a_i \in \mathcal{A}_i$ we construct the object \hat{Q} :

$$\hat{Q}_i(s, a_i) = \frac{1}{k} \sum_{j=1}^k Q_i(s, a_i, \mathbf{a}_i^{(j)}); \quad \mathbf{a}_i^{(j)} \sim \pi(\mathbf{a}_{-i} | \tau_{-i}). \quad (2)$$

We now describe the implementation details of Actor-Critic algorithm using the critic policy embedding procedure, along with pseudocode in Algorithm 1:

1. Augment the critic Q to accommodate joint action, i.e., $Q(s^t, a_i^t, \mathbf{a}_{-i}^{t(j)})$.
2. Each agent i communicates its policy π_i and its local observation τ_i^t to other agents.
3. Upon arrival to state s^t each agent i samples other agents’ actions given their local observations, k times using other agents’ policies $a_j \sim \pi_j(a_j | \tau_j^t)$. This produces joint samples of the actions $\{\mathbf{a}_{-i}^{t(j)}\}_{j=1}^k$ for each time step t .
4. Each agent uses this to approximate the function $\tilde{Q}_i(s^t, a_i^t) = \frac{1}{k} \sum_{j=1}^k Q(s^t, a_i^t, \mathbf{a}_{-i}^{t(j)}) \approx \hat{Q}_i(s^t, a_i^t)$, embedding the behaviour of other agents.
5. Agent i uses \tilde{Q}_i as the critic to update its policy using the chosen policy gradient algorithm.
6. Return to 2 and repeat until termination.

In our experiments, we use a value-function style critic, where $Q(s^t, a_i^t, \mathbf{a}_{-i}^{t(j)}) = r_t + \gamma V(s^t, \mathbf{a}_{-i}^{t(j)})$ and $V(s^t, \mathbf{a}_{-i}^{t(j)})$ is approximated via a deep neural network. In this case, it is enough to marginalise the next step values function. To perform policy updates, we use PPO updates (Schulman et al. 2017). We apply PERLA to two cases, one which involves a base learner whose critic input captures global information (MAPPO (Yu et al. 2021a)) and another base learner whose critic input is only local observations (IPPO) (in both cases, PERLA makes use of shared global state information during training). This gives rise to **PERLA MAPPO** and **PERLA IPPO** algorithms respectively.

4 Theoretical Analysis

In this section, we perform a detailed theoretical analysis of PERLA. Here, we derive theoretical results that establish

Algorithm 1: PERLA MAPPO/IPPO

Input: Joint-policy π , critic parameters ϕ , policy parameters θ , environment E , number of marginalisation samples K

Output: Optimised joint-policy π

- 1 Instantiate critic Q_ϕ that takes as input state s , action a_i and joint-action a_{-i} // Equation 2
- 2 Rollout π in E to obtain data

$$D = (s^0, a^1, r^1, \dots, s^{T-1}, a^T, r^T)$$
- 3 **for** $t \leftarrow 0$ **to** T **do**
- 4 **for** each agent i **do**
- 5 Generate K samples of joint-actions

$$\{a_{-i}^{t(j)} \sim \pi_{-i}(\tau^t)\}_{j=1}^K$$
- 6 Compute TD-error

$$\delta_i = \frac{1}{K} \sum_{j=1}^K Q_\rho(s^{t-1}, a_{-i}^{t-1(j)}, a_i) - (r + \gamma \frac{1}{K} \sum_{j=1}^K Q_\rho(s^t, a_{-i}^{t(j)}, a_i))$$
- 7 over sampled joint-actions for each agent // Equation 2
- 8 Update critic parameters ρ with δ_i
- 9 Update i th agent's policy parameters θ_i with advantages given by δ_i , using PPO update

the key benefits of PERLA, namely that it vastly reduces variance of the key estimates used in training. We begin with a result that quantifies the reduction of variance when using \hat{Q}_i instead of Q_i . We defer all proofs to the Appendix.

Theorem 1. *The variance of marginalised Q-function \tilde{Q}_i is smaller than that of the non-marginalised Q-function Q_i for any $i \in \mathcal{N}$, that is to say: $\text{Var}(Q_i(s, \mathbf{a})) \geq \text{Var}(\tilde{Q}_i(s, a_i))$. Moreover, for the approximation to the marginalised Q-function (c.f. Equation 2) the following relationship holds:*

$$\text{Var}(\hat{Q}_i(s, a_i)) = \frac{1}{k} \text{Var}(Q_i(s, a_{-i}, a_i)) + \frac{k-1}{k} \text{Var}(\tilde{Q}_i(s, a_i)).$$

Therefore for $k = 1$ we get that the approximation has the same variance as the non-marginalised Q-function. However, for any $k > 1$ the approximation to marginalised Q-function has smaller variance than the non-marginalised Q-function. Therefore marginalisation procedure of PERLA can essentially be used as a variance reduction technique. Let us now analyse how this framework can be applied to enhance multi-agent policy gradient algorithm, which is known to suffer from high variance in its original version.

In the policy gradient algorithms, we assume a fully cooperative game which avoids the need to add the agent indices to the state-action and state-value functions since the agents have identical rewards. The goal of each agent is therefore to maximise the expected return from the initial state defined as $\mathcal{J}(\theta) = \mathbb{E}_{s_0 \sim p(s_0)}[v(s_0)]$, where $p(s_0)$ is the distribution of initial states and $\theta = (\theta_1^T, \dots, \theta_N^T)^T$ is the concatenated vector consisting of policy parameters for all agents. The following well-known theorem establishes the gradient of $\mathcal{J}(\theta)$ with respect to the policy parameters.

Theorem 2 (MARL Policy Gradient (Zhang et al. 2018)).

$$\nabla_{\theta_i} \mathcal{J}(\theta) = \mathbb{E} \left[\sum_{t=0}^{\infty} \gamma^t Q(s^t, a_{-i}^t, a_i^t) \nabla_{\theta_i} \log \pi_i(a_i^t | \tau_i^t) \right].$$

Therefore, to calculate the gradient with respect to policy parameters, it is necessary to make use of the state-action-values. In practice, it can be estimated by a function approximator, which gives rise to Actor-Critic methods (Konda and Tsitsiklis 1999). In MARL, one can either maintain a centralised critic that provides state-action-value for the i th agent using the knowledge of the other agents' actions or introduce a decentralised critic that does not take actions of others (in its inputs). This gives rise to the centralised training decentralised execution (CT-DE) \mathbf{g}_i^C and decentralised \mathbf{g}_i^D gradient estimators respectively, as defined below.

$$\mathbf{g}_i^C := \sum_{t=0}^{\infty} \gamma^t Q(s^t, a_{-i}^t, a_i^t) \nabla_{\theta_i} \log \pi_i(a_i^t | \tau_i^t), \quad (3)$$

$$\mathbf{g}_i^D := \sum_{t=0}^{\infty} \gamma^t \tilde{Q}(s^t, a_i^t) \nabla_{\theta_i} \log \pi_i(a_i^t | \tau_i^t), \quad (4)$$

where $Q(s^t, a_{-i}^t, a_i^t)$ and $\tilde{Q}(s^t, a_i^t)$ are the CT-DE and decentralised critics respectively. In PERLA Actor-Critic algorithms (such as in Algorithm 1) we utilise a third estimator - the PERLA estimator given below:

$$\mathbf{g}_i^P := \sum_{t=0}^{\infty} \gamma^t \hat{Q}(s^t, a_i^t) \nabla_{\theta_i} \log \pi_i(a_i^t | \tau_i^t),$$

where $\hat{Q}(s^t, a_i^t)$ is the Monte-Carlo approximation of $\tilde{Q}(s^t, a_i^t)$. Note that in this approach we maintain a centralised critic $Q(s^t, a_{-i}^t, a_i^t)$, therefore the approximation to the marginalised Q-function is obtained using $\hat{Q}(s^t, a_i^t) = \frac{1}{k} \sum_{j=1}^k Q(s^t, a_i^t, a_{-i}^{t(j)})$, where $a_{-i}^{t(j)} \sim \pi_{-i}(a_{-i}^t | \tau_i^t)$. The PERLA estimator is equal in expectation to the CT-DE estimator as stated by the following Theorem.

Theorem 3. *Given the same (possibly imperfect) critic, the estimators \mathbf{g}_i^C and \mathbf{g}_i^P have the same expectation, that is:*

$$\mathbb{E}[\mathbf{g}_i^C] = \mathbb{E}[\mathbf{g}_i^P].$$

Therefore, whenever the critic provides the true Q-value, PERLA estimator is an unbiased estimate of the policy gradient (which follows from Theorem 2). However, although the CT-DE and PERLA estimators have the same expectations, the PERLA estimator enjoys significantly lower variance. Similar to the analysis in (Kuba et al. 2021), let us study the excess variance those two estimators have over the decentralised estimator. Let B_i be the upper bound on the gradient norm of i th agent, i.e. $B_i = \sup_{s, a} \|\nabla_{\theta_i} \log \pi_i(a_i | s)\|$ and C be the upper bound on the Q-function, i.e. $C = \sup_{s, a} Q(s, a)$.

We can now present two theorems showing the effectiveness of PERLA estimator for policy gradients.

Theorem 4. *Given true Q-values, the difference in variances between the decentralised and PERLA estimators admits the following bound:*

$$\text{Var}(\mathbf{g}_i^P) - \text{Var}(\mathbf{g}_i^D) \leq \frac{1}{k} \frac{B_i^2 C^2}{1 - \gamma^2}.$$

Theorem 5. Given true Q -values, the difference in variances between the decentralised and CT-DE estimators admits the following bound:

$$\text{Var}(\mathbf{g}_i^C) - \text{Var}(\mathbf{g}_i^D) \leq \frac{B_i^2 C^2}{1 - \gamma^2}.$$

Therefore, we can see that with $k = 1$ the bound on excess variance of the PERLA estimator is the same as for the CT-DE estimator, but as $k \rightarrow \infty$, the variance of PERLA estimator matches the one of the fully decentralised estimator. However, this is done while still maintaining a centralised critic, unlike in the fully decentralised case. It turns out that the presence of centralised critic is critical, as it allows us to guarantee the converge of an algorithm to a local optimum with probability 1. The result is stated by the next Theorem.

Theorem 6. Under the standard assumptions of stochastic approximation theory (Konda and Tsitsiklis 1999), an Actor-Critic algorithm using \mathbf{g}_i^P or \mathbf{g}_i^C as a policy gradient estimator, converges to a local optimum with probability 1, i.e.

$$P \left(\lim_{k \rightarrow \infty} \|\nabla_{\theta_i} \mathcal{J}(\theta^k)\| = 0 \right) = 1,$$

where θ^k is the value of vector θ obtained after the k th update following the policy gradient.

Proof sketch. We present a proof sketch here and defer the full proof to Appendix I.

The proof consists of showing that a multi-agent Actor-Critic algorithm using policy gradient estimate \mathbf{g}_i^P or \mathbf{g}_i^C is essentially a special case of single-agent Actor-Critic. \square

Note that because the decentralised critic does not allow us to query the state-action-value for joint action of all agents, a decentralised actor-critic using \mathbf{g}_i^D as policy gradient estimate is not equivalent to the single-agent version and we cannot establish convergence for it. Therefore, our PERLA estimator enjoys both the low variance property of the decentralised estimator and the convergence guarantee of the CT-DE one. Additionally, having a centralised critic yields better performance in practice in environments with strong interactions between agents (Kok and Vlassis 2004).

5 Experiments

We ran a series of experiments in *Large-scale Matrix Games* (Son et al. 2019), *Level-based Foraging* (LBF) (Christianos, Schäfer, and Albrecht 2020), *Multi-agent Mujoco* (de Witt et al. 2020b) and the *StarCraft II Multi-agent Challenge* (SMAC) (Samvelyan et al. 2019)² to test if PERLA: **1.** Improves overall performance of MARL base learners. **2.** Enables efficient scaling in the number of agents. **3.** Reduces variance of value function estimates. In all tasks, we compared the performance of PERLA against MAPPO (Yu et al. 2021a) and IPPO (de Witt et al. 2020a). Here, we report average training results across multiple maps for LBF and SMAC. Further performance comparisons across these maps

²The specific maps/variants used of each of these environments is given in Section B of the Appendix)

| | b_1 | b_2 | b_3 |
|-------|----------|-------|-------|
| a_1 | 8 | -12 | -12 |
| a_2 | -12 | 0 | 0 |
| a_3 | -12 | 0 | 0 |

Table 1: Payoff matrix for 2 agents and 3 actions each.

are deferred to the Appendix. Lastly, we ran a suite of ablation studies which we deferred to the Appendix.

We used the codebase accompanying the MARL benchmark study in Papoudakis et al. (2021) to implement PERLA on top IPPO (Schulman et al. 2017) and MAPPO (Yu et al. 2021a). IPPO is a decentralised learning algorithm, while MAPPO follows the CT-DE paradigm. Implementing PERLA on both widely used training paradigms enables us to examine the impact of PERLA in each case. Hyperparameters were tuned using simple grid-search, and the values over which we tuned them are presented in Table 3 in the Appendix. All results are statistics of the metric being measured over 3 random seeds unless otherwise stated. In our plots dark lines represent the mean across the seeds, while shaded areas represent 95% confidence intervals.

5.1 Performance Analysis

We conducted experiments to ascertain if PERLA yields performance improvements to base MARL algorithms to which it is added as claimed.

Large-Scale Matrix Games. To demonstrate PERLA’s ability to handle various reward structure and scale efficiently we first tested its performance in a set of variants of the hard matrix game proposed in (Son et al. 2019) given in Fig. 1. The game contains multiple stable points and a strongly attracting equilibrium (a_1, b_1) .

To ensure sufficient data collection in the joint action space, we adopted uniform data distribution in batch learning techniques. With this fixed dataset, we can compare the optimality of PERLA and baselines from an optimisation perspective. We use 500 training iterations and average the results of $[0 - 10]$ random seeds in each method. As shown in Table 1, policy-based methods (MAPPO and IPPO) and leading value-based methods (MAIC, QPLEX (Wang et al. 2020) and WQMIX (Rashid et al. 2020)) achieve optimal performance in the initial settings (2 agents with 3 available actions), while other algorithms achieve suboptimal outcomes. When scaling with more agents and larger action space, only PERLA can maintain the optimal performance nearly across all action sizes. This is because PERLA enables agents to maintain estimates that account for other agents’ actions. Other policy-based methods (MAPPO and IPPO) only consider states as inputs in critic network, without considering agents’ actions. Most of value-based baselines (except for QTRAN) are strictly restricted by IGM consistency, which may not be suitable for complex domains.

Level-based Foraging. Figure 2 shows learning curves averaged across all LBF maps that we ran (the full list of maps is given in the Appendix E). As shown in the plots, PERLA enhances the base algorithm. Compared to standard IPPO, PERLA_IPPO learns significantly faster: the PERLA_IPPO achieves evaluation of return of 0.6

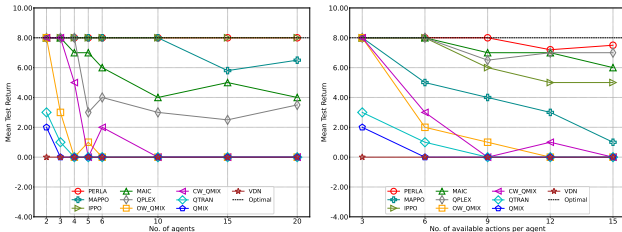


Figure 1: Results of scaling with more agents (bottom left) and larger action space (bottom right) in cooperative matrix game extensions of the matrix game (Table 1).

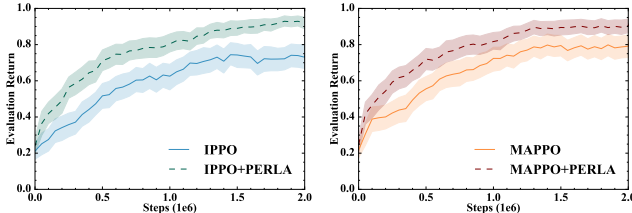


Figure 2: Average performance over all tested LBF maps of IPPO, PERLA_IPPO (left); MAPPO, PERLA_MAPPO (right). PERLA improves sample efficiency (better performance faster) and performance of the final policy.

by about 300k training steps while standard IPPO only achieves the same performance after 1,000k steps. Crucially, PERLA_IPPO learns superior policies at the end of training (achieving returns of approximately 0.8) compared to standard IPPO (which achieves around 0.65 in returns after training) which is around a 20% increase. Similarly, PERLA_MAPPO enhances standard MAPPO but does so to a lesser extent achieving a return of 0.6 after approximately 300k steps while standard MAPPO requires about 600,000 steps to achieve the same performance.

StarCraft II Multi-agent Challenge. Figure 3 shows averaged performance of base IPPO and MAPPO and their respective PERLA variants over a wide range of SMAC maps from all difficulty levels. At regular intervals during training, we ran several evaluation episodes and tracked the median win-rate. The learning curves are then generated by computing the mean of the median win rate. SMAC maps are richly diverse and vary in the number of agents to control, density of environment reward, degree of coordination required, and (partial)-observability. Therefore, aggregated and averaged performance over all maps gives us a fairly robust understanding of the effects of PERLA. As with LBF, PERLA enhances the performance of IPPO to a much greater degree than MAPPO. However, there are clear gains with both algorithms. In both cases, the PERLA variants of the algorithms are more sample efficient and converge to better overall policies (within the training budget).

Multi-agent Mujoco.

To study PERLA’s capabilities in complex settings that require both scalability and coordination, we compared its performance with the aforementioned baselines on three tasks in multi-agent Mujoco: Walker 2×3, Hopper 3×1, and Swimmer 2×1. In Fig. 13 (see Appendix), we report our re-

sults showing the performance of PERLA against leading MARL baselines. We ran 6 runs of each algorithm. Fig. 13 we can see PERLA outperforms IPPO and MAPPO on all three tasks. By enabling agents to maintain estimates that account for other agents’ actions, PERLA achieves more accurate value estimation with the variance reduction, therefore establishing more efficient learning.

PERLA eliminates IPPO failure modes.

Despite independent learners (IL) being scalable and quick to train, IL can fail to achieve coordination between agents and occasionally fail to solve the task altogether. In Section 1, we claimed PERLA induces coordination and can minimise failure modes exhibited by IL. To test this claim, we counted the number of maps where an algorithms return at evaluation or test win-rate was below 0.1 at the end of training. Figure 4 shows the frequency of training failures over a range of SMAC and LBF maps (see Appendix B) for IL (IPPO), CL (MAPPO), and PERLA_IPPO. As in shown in Figure 4, *Perlasing* IPPO eliminates the occurrence of failure modes for IPPO as claimed. Crucially, as we later show, PERLA has highly efficient scalability benefits while eliminating the failure modes of IL.

PERLA boosts performance in fully observable settings.

Perlisation of IL methods introduces global state information during training (while training with a Q function whose input space is local observations). In some cases, accessing global state (GS) information can improve performance during training. To verify that PERLA delivers vast benefits beyond providing access to global information, we ran PERLA_IPPO against MAPPO and IPPO on a variant of LBF which is fully observable (i.e. each agent’s local observation provides full information about the full system state). Figure 5 shows performance of of both IPPO (GS) and PERLA_IPPO (GS) when the algorithms now have access to global state information. PERLA_IPPO outperforms IPPO indicating the performance benefits of *Perlasing* IPPO extend beyond providing GS information.

5.2 Scaling Analysis

Scaling efficiently to large systems (i.e. systems with many agents and large action spaces) is a major challenge for MARL. In Sec. 1, we claimed the PERLA framework enables MARL to scale efficiently. To test this claim, we investigated PERLA’s scaling ability in our large scale matrix games (described above) and LBF. In matrix games, we demonstrated PERLA’s ability to efficiently scale across both dimensions namely games varied by i) the number of agents $N = 2, 3, 4, 5, 6, 10, 15, 20$ and ii) the cardinality of the agents’ action sets $|\mathcal{A}_i| = 3, 6, 9, 12, 15$. In each case, we retained the setup that reward agents with a score of 8 only when all agents choose the first action.

We then tested this claim in LBF where we varied the number of agents in the system. Fig. 6 shows PERLA_IPPO’s percentage performance gains over IPPO and MAPPO. As shown, the performance gains monotonically increase with the number of agents yielding over 1000% improvement in systems with 8 agents.

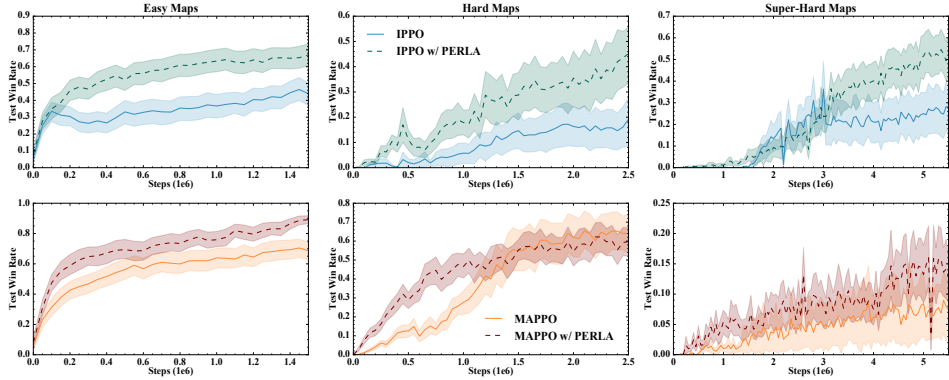


Figure 3: Average performance over *all* SMAC maps for IPPO, PERLA_IPPO (top); MAPPO, PERLA_MAPPO (bottom). PERLA enhances the base method both in terms of sample efficiency (better performance, faster) and final performance.

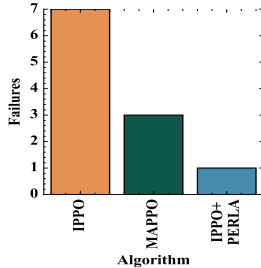


Figure 4: Learning failure frequencies (across all SMAC and LBF maps). PERLA_IPPO vastly reduces occurrences of learning failure and outperforms the CL method, MAPPO.

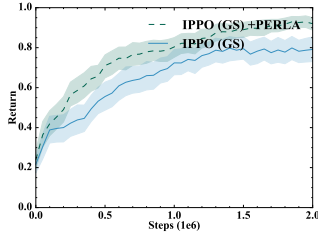


Figure 5: Learning performances of IPPO and PERLA_IPPO with access to the global state (GS). PERLA_IPPO outperforms IPPO by over 15%.

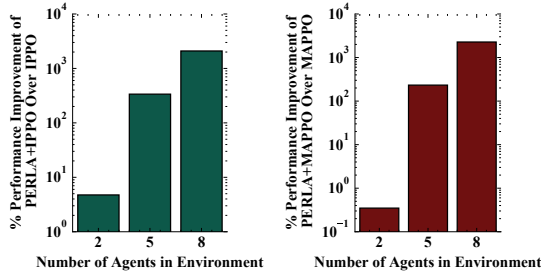


Figure 6: Performance improvement (%) after training of PERLA_IPPO over IPPO (left) and MAPPO (right) as the number of agents (N) increases. For $N = 8$, PERLA_IPPO yields over +1000% performance gains over both baselines.

5.3 Variance Analysis

In Sec. 4, we proved that PERLA reduces the variance of VF estimators. To show this empirically, we reported the cumulative TD-errors (which serve as proxies for the value estimates (Tamar, Di Castro, and Mannor 2016)) over the course of training in LBF 20×20 10p3f over 5 seeds.

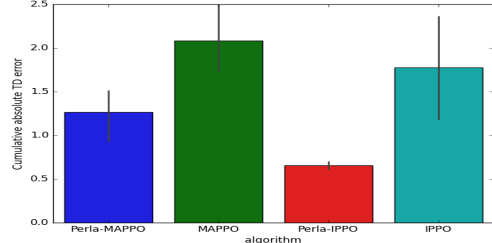


Figure 7: Comparison of cumulative TD errors on the LBF task. Shown with 0.95 confidence intervals over 5 seeds.

6 Conclusion

MARL estimators suffer from high variance due to a number of sources of randomness. This hinders learning and reduces the sample efficiency of MARL methods. Secondly, many leading CT-DE algorithms avoid exponential scaling complexity at the expense of employing representational constraints that impose strong restrictions. Despite the popularity of the CT-DE paradigm, its efficacy is heavily constrained by limits imposed by these challenges. On the other hand, IL often depend on random instances of coordination to solve tasks which can lead to poor sample efficiency and learning failures. Consequently, scalability and efficient learning are key challenges in MARL research.

We introduced PERLA, a plug & play enhancement tool that enables MARL to scale efficiently while inducing sample efficient, coordinated learning among MARL agents. Our theory and empirical analyses show that PERLA reduces the variance of VF estimators which is critical for efficient learning. By introducing a *policy embedding protocol* which factors in the behaviour of other agents in the

critic functional representation, PERLA avoids joint action input spaces to train MARL critics. In this way, PERLA enables MARL to exhibit the scalability benefits of IL while achieving coordinated learning, often required to achieve optimal performance. This unlocks the capacity for coordinated behaviours among MARL agents whose critic structure resembles that of IL agents. In doing so, PERLA powerfully bridges the gap between MARL and single agent RL.

References

Christianos, F.; Schäfer, L.; and Albrecht, S. V. 2020. Shared Experience Actor-Critic for Multi-Agent Reinforcement Learning. In *Advances in Neural Information Processing Systems (NeurIPS)*.

de Witt, C. S.; Gupta, T.; Makoviichuk, D.; Makoviychuk, V.; Torr, P. H.; Sun, M.; and Whiteson, S. 2020a. Is Independent Learning All You Need in the StarCraft Multi-Agent Challenge? *arXiv preprint arXiv:2011.09533*.

de Witt, C. S.; Peng, B.; Kamienny, P.-A.; Torr, P.; Böhmer, W.; and Whiteson, S. 2020b. Deep multi-agent reinforcement learning for decentralized continuous cooperative control. *arXiv preprint arXiv:2003.06709*.

Deng, X.; Li, Y.; Mgundi, D. H.; Wang, J.; and Yang, Y. 2021. On the complexity of computing markov perfect equilibrium in general-sum stochastic games. *arXiv preprint arXiv:2109.01795*.

Foerster, J. N.; Chen, R. Y.; Al-Shedivat, M.; Whiteson, S.; Abbeel, P.; and Mordatch, I. 2018a. Learning with Opponent-Learning Awareness. In *AAMAS'18*, 122–130.

Foerster, J. N.; Farquhar, G.; Afouras, T.; Nardelli, N.; and Whiteson, S. 2018b. Counterfactual multi-agent policy gradients. In *Thirty-second AAAI conference on artificial intelligence*.

Grover, A.; Al-Shedivat, M.; Gupta, J. K.; Burda, Y.; and Edwards, H. 2018. Learning Policy Representations in Multiagent Systems. In *ICML'18*, volume 80, 1797–1806.

Gu, S.; Lillicrap, T.; Ghahramani, Z.; Turner, R. E.; and Levine, S. 2016. Q-prop: Sample-efficient policy gradient with an off-policy critic. *arXiv preprint arXiv:1611.02247*.

Gupta, J. K.; Egorov, M.; and Kochenderfer, M. 2017. Cooperative multi-agent control using deep reinforcement learning. In *International conference on autonomous agents and multiagent systems*, 66–83. Springer.

Hong, Z.; Su, S.; Shann, T.; Chang, Y.; and Lee, C. 2018. A Deep Policy Inference Q-Network for Multi-Agent Systems. In *AAMAS'18*, 1388–1396.

Kok, J. R.; and Vlassis, N. 2004. Sparse cooperative Q-learning. In *Proceedings of the twenty-first international conference on Machine learning*, 61.

Konda, V.; and Tsitsiklis, J. 1999. Actor-critic algorithms. *Advances in neural information processing systems*, 12.

Kuba, J. G.; Wen, M.; Meng, L.; Zhang, H.; Mgundi, D.; Wang, J.; Yang, Y.; et al. 2021. Settling the variance of multi-agent policy gradients. *Advances in Neural Information Processing Systems*, 34: 13458–13470.

Lowe, R.; Wu, Y. I.; Tamar, A.; Harb, J.; Pieter Abbeel, O.; and Mordatch, I. 2017. Multi-agent actor-critic for mixed cooperative-competitive environments. *Advances in neural information processing systems*, 30.

Mahajan, A.; Rashid, T.; Samvelyan, M.; and Whiteson, S. 2019. Maven: Multi-agent variational exploration. *arXiv preprint arXiv:1910.07483*.

Mgundi, D.; Jennings, J.; and de Cote, E. M. 2018. Decentralised learning in systems with many, many strategic agents. In *Thirty-Second AAAI Conference on Artificial Intelligence*.

Mgundi, D.; Wu, Y.; Du, Y.; Yang, Y.; Wang, Z.; Li, M.; Wen, Y.; Jennings, J.; and Wang, J. 2021a. Learning in Nonzero-Sum Stochastic Games with Potentials. *arXiv preprint arXiv:2103.09284*.

Mgundi, D. H.; Jafferjee, T.; Wang, J.; Perez-Nieves, N.; Slumbers, O.; Tong, F.; Li, Y.; Zhu, J.; Yang, Y.; and Wang, J. 2021b. LIGS: Learnable Intrinsic-Reward Generation Selection for Multi-Agent Learning. *arXiv preprint arXiv:2112.02618*.

Papoudakis, G.; Christianos, F.; Schäfer, L.; and Albrecht, S. V. 2021. Benchmarking Multi-Agent Deep Reinforcement Learning Algorithms in Cooperative Tasks. In *Proceedings of the Neural Information Processing Systems Track on Datasets and Benchmarks (NeurIPS)*.

Peng, B.; Rashid, T.; de Witt, C. A. S.; Kamienny, P.-A.; Torr, P. H.; Böhmer, W.; and Whiteson, S. 2020. FACMAC: Factored Multi-Agent Centralised Policy Gradients. *arXiv preprint arXiv:2003.06709*.

Peng, P.; Wen, Y.; Yang, Y.; Yuan, Q.; Tang, Z.; Long, H.; and Wang, J. 2017. Multiagent bidirectionally-coordinated nets: Emergence of human-level coordination in learning to play starcraft combat games. *arXiv preprint arXiv:1703.10069*.

Raileanu, R.; Denton, E.; Szlam, A.; and Fergus, R. 2018. Modeling Others using Oneself in Multi-Agent Reinforcement Learning. In *ICML'18*, volume 80, 4254–4263.

Rashid, T.; Farquhar, G.; Peng, B.; and Whiteson, S. 2020. Weighted qmix: Expanding monotonic value function factorisation for deep multi-agent reinforcement learning. *arXiv preprint arXiv:2006.10800*.

Rashid, T.; Samvelyan, M.; Schroeder, C.; Farquhar, G.; Foerster, J.; and Whiteson, S. 2018. Qmix: Monotonic value function factorisation for deep multi-agent reinforcement learning. In *International Conference on Machine Learning*, 4295–4304. PMLR.

Samvelyan, M.; Rashid, T.; De Witt, C. S.; Farquhar, G.; Nardelli, N.; Rudner, T. G.; Hung, C.-M.; Torr, P. H.; Foerster, J.; and Whiteson, S. 2019. The starcraft multi-agent challenge. *arXiv preprint arXiv:1902.04043*.

Schulman, J.; Wolski, F.; Dhariwal, P.; Radford, A.; and Klimov, O. 2017. Proximal Policy Optimization Algorithms. *CoRR*, abs/1707.06347.

Son, K.; Kim, D.; Kang, W. J.; Hostallero, D. E.; and Yi, Y. 2019. Qtran: Learning to factorize with transformation for cooperative multi-agent reinforcement learning. In *International Conference on Machine Learning*, 5887–5896. PMLR.

Tamar, A.; Di Castro, D.; and Mannor, S. 2016. Learning the variance of the reward-to-go. *The Journal of Machine Learning Research*, 17(1): 361–396.

Wang, J.; Ren, Z.; Liu, T.; Yu, Y.; and Zhang, C. 2020. Qplex: Duplex dueling multi-agent q-learning. *arXiv preprint arXiv:2008.01062*.

Willi, T.; Treutlein, J.; Letcher, A.; and Foerster, J. N. 2022. COLA: Consistent Learning with Opponent-Learning Awareness.

Yang, Y.; and Wang, J. 2020. An Overview of Multi-Agent Reinforcement Learning from Game Theoretical Perspective. *arXiv preprint arXiv:2011.00583*.

Yang, Y.; Wen, Y.; Wang, J.; Chen, L.; Shao, K.; Mguni, D.; and Zhang, W. 2020. Multi-agent determinantal q-learning. In *International Conference on Machine Learning*, 10757–10766. PMLR.

Yu, C.; Velu, A.; Vinitsky, E.; Wang, Y.; Bayen, A.; and Wu, Y. 2021a. The surprising effectiveness of mappo in cooperative, multi-agent games. *arXiv preprint arXiv:2103.01955*.

Yu, X.; Jiang, J.; Jiang, H.; and Lu, Z. 2021b. Model-Based Opponent Modeling. *CoRR*, abs/2108.01843.

Zhang, K.; Yang, Z.; Liu, H.; Zhang, T.; and Basar, T. 2018. Fully decentralized multi-agent reinforcement learning with networked agents. In *International Conference on Machine Learning*, 5872–5881. PMLR.

Zhou, M.; Luo, J.; Villella, J.; Yang, Y.; Rusu, D.; Miao, J.; Zhang, W.; Alban, M.; Fadakar, I.; Chen, Z.; et al. 2020. Smarts: Scalable multi-agent reinforcement learning training school for autonomous driving. *arXiv preprint arXiv:2010.09776*.

Appendix

A Ablation Study - Number of Samples Used in Marginalization

We ran an ablation study over the number of samples required to marginalise Q_i to obtain \hat{Q} . We selected three tasks from Level-based Foraging at random: Foraging-5x5-2p-1f-coop, Foraging-10x10-5p-3f, and Foraging-10x10-3p-5f. We ran PERLA_IPPO on these maps with a range of values for K for three seeds each. Figure 8 shows the area-under-the-curve averaged across seeds and across the three maps versus K . As expected, the general trend is that more samples yields better performance. PERLA_IPPO with $K = 100$ is significantly better than PERLA_IPPO with $K = 5$. However this trend discontinues beyond $K = 250$ — the algorithm performs slightly worse than $K = 100$ indicating that increasing the number of samples does not improve performance.

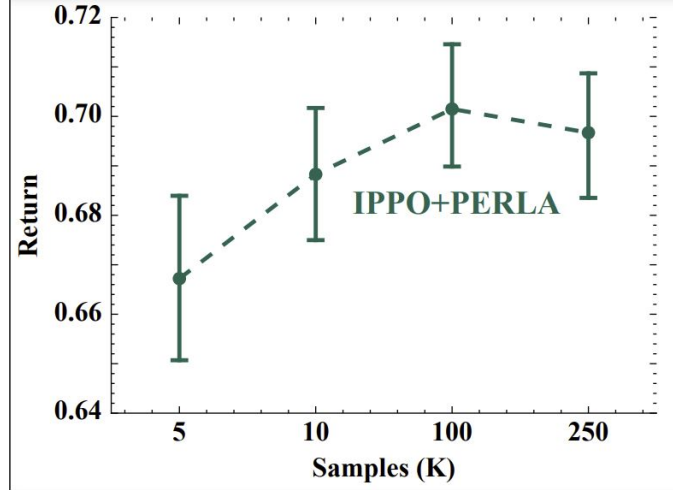


Figure 8: Ablation on K , the number of samples used to marginalise Q_i . As expected, the overall trend in the plots suggests that more samples are better.

B Learning Curves on Level-Based Foraging

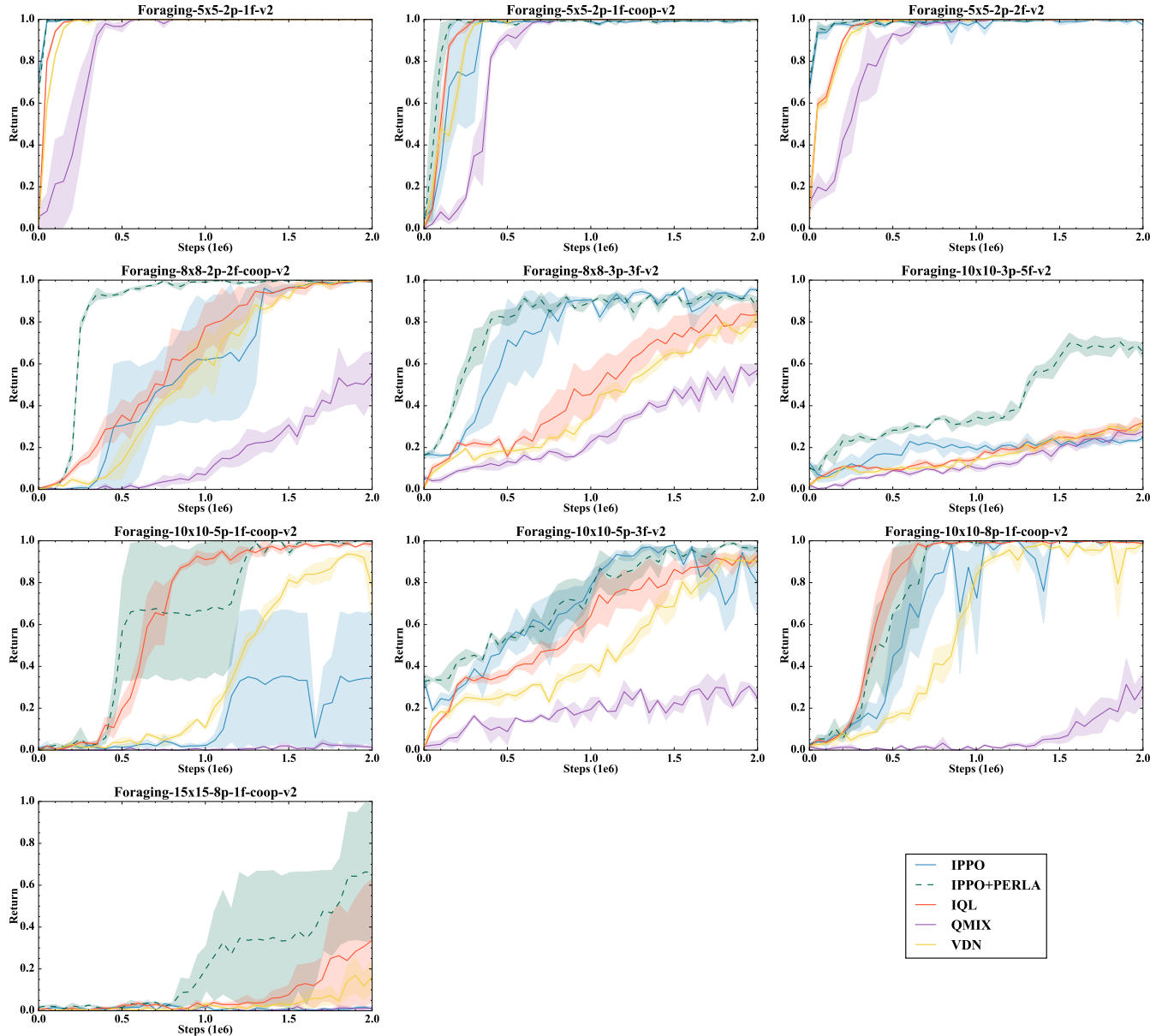


Figure 9: Learning curves across all tested Level-Based Foraging maps for PERLA_IPPO and baselines. PERLA_IPPO outperforms all baselines.

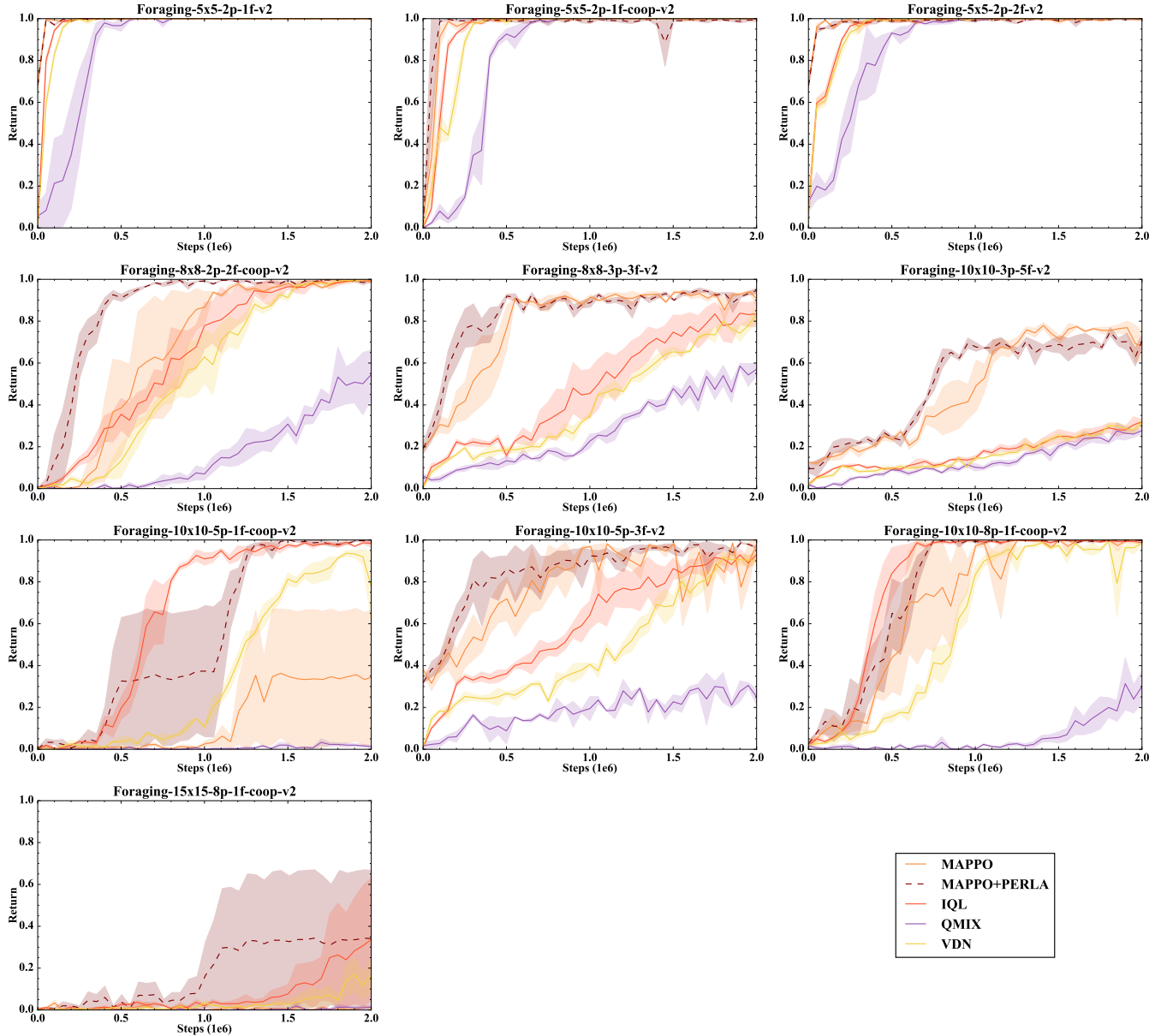


Figure 10: Learning curves across all tested Level-Based Foraging maps for PERLA_MAPPO. PERLA_MAPPO outperforms all baselines.

C Learning Curves on Starcraft Multi-agent Challenge

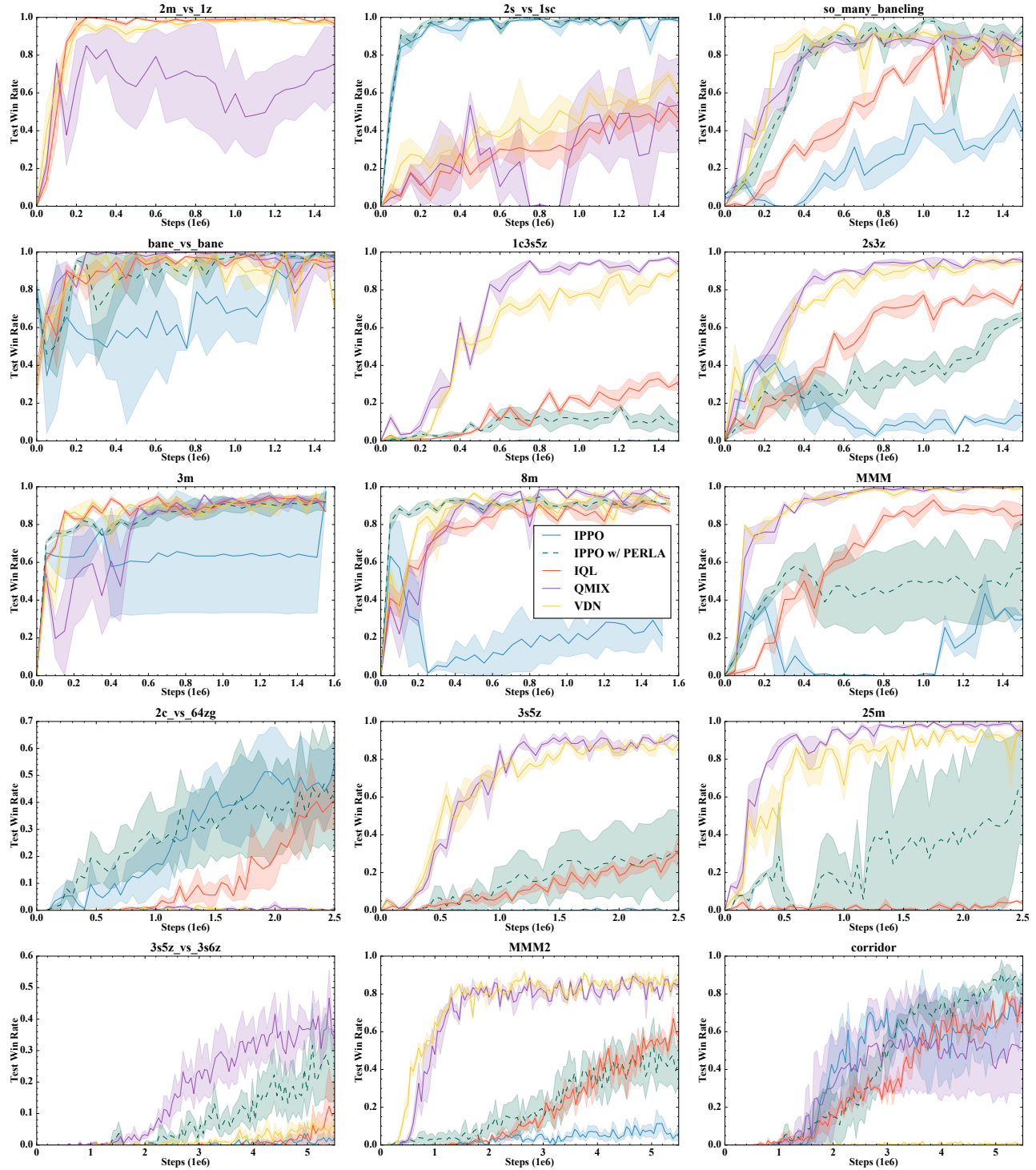


Figure 11: Learning curves across all tested StarCraft Challenge maps for MAPPO and PERLA_MAPPO. In each case, PERLA_MAPPO outperforms MAPPO.

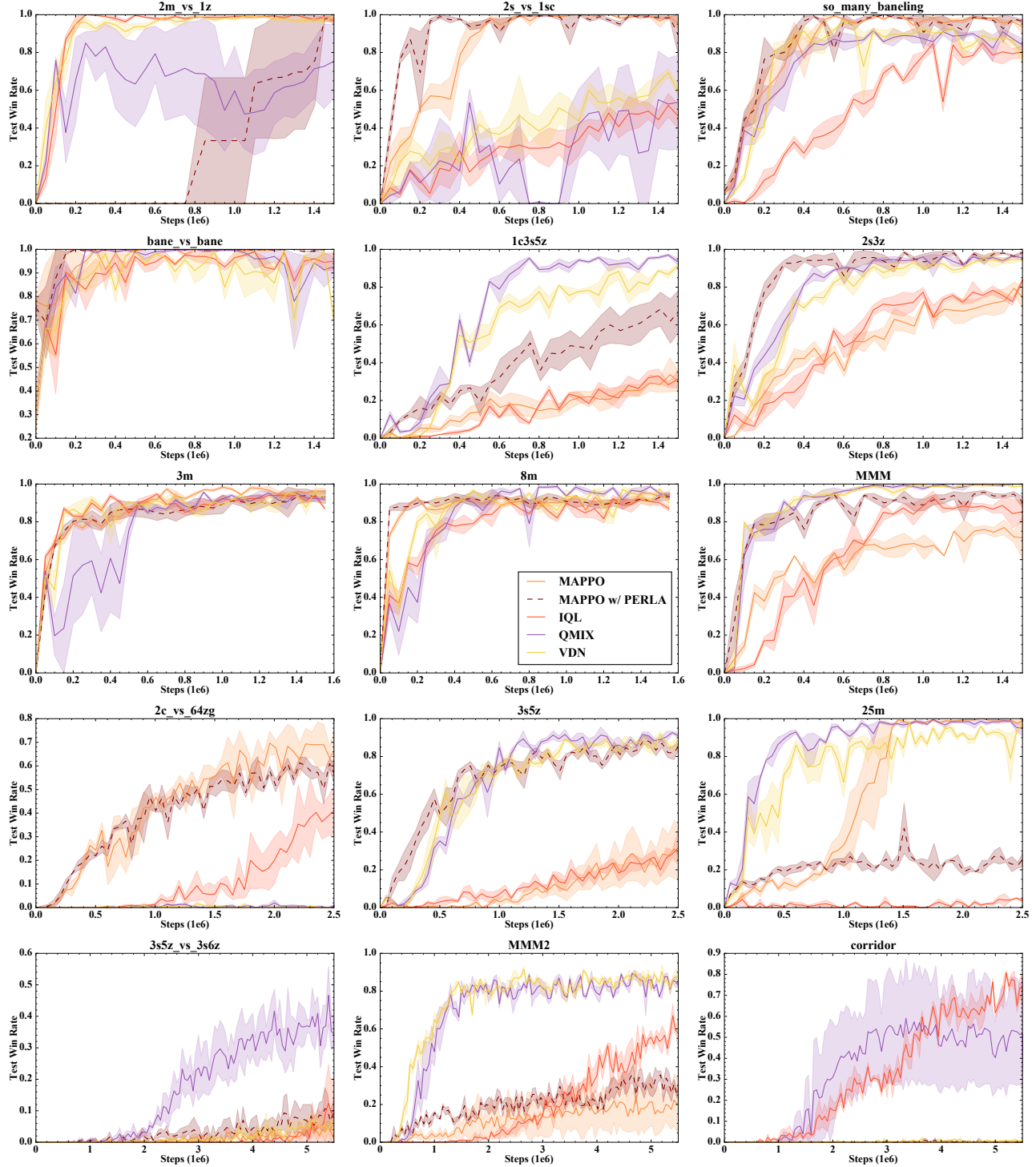


Figure 12: Learning curves across all tested StarCraft Challenge maps for MAPPO and MAPPO with PERLA. In each case, PERLA_MAPPO outperforms MAPPO.

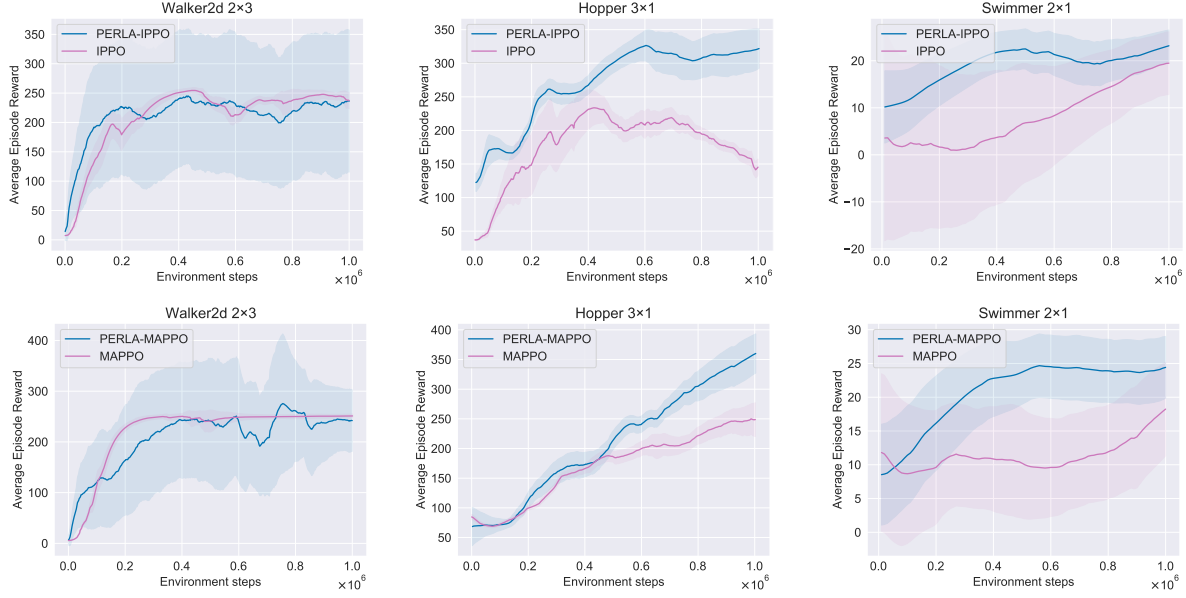


Figure 13: Comparisons of PERLA variants versus base learners on Multi-agent Mujoco tasks.

D Computing Resources and Hyperparameters

D.1 Computing Resources

All experiments (including hyperparameter search) were run on machines equipped as described in Table 2. We used multiple such machines in parallel to complete all runs.

| Component | Description |
|-----------|-----------------------------------|
| CPU | Intel Core i9-9900X CPU @ 3.50GHz |
| GPU | Nvidia RTX 2080 |
| Memory | 64 GB DDR4 |

Table 2: Specifications of machines used to run empirical component of this paper.

D.2 Hyperparameters

We used the implementation of (Papoudakis et al. 2021) for the baseline algorithms as well as the foundation upon which we implemented the *PERLAISED* version of IPPO and MAPPO. For the baseline algorithms, we re-used the optimal hyperparameters reported by (Papoudakis et al. 2021). To optimise PERLA_IPPO and PERLA_MAPPO, for each environment, we sampled a small number of tasks and used simple grid-search to optimise selected hyperparameters. The combination of hyperparameters that achieved maximum Return or Test Win-Rate were then used in the runs of all remaining tasks. Table 3 shows the hyperparameters optimised and the range of values evaluated.

| Hyperparameter | Range |
|--|---|
| Hidden Dimension | [64, 128, 256] |
| Learning Rate | [3e-4, 5e-4] |
| Network Type | [Fully-connected, Gated Recurrent Network] |
| Reward Standardisation | [False, True] |
| Entropy Coefficient | [1e-3 1e-2 1e-1] |
| Target network update | [Hard update every 200 steps, Soft update of 0.01 per step] |
| Number of steps for calculating Return | [5, 10] |
| Number of PERLA samples (K) | [10, 100] |

Table 3: Hyperparameters and range of values evaluated to optimise *PERLAISED* variants of IPPO and MAPPO.

E LBF experiments

E.1 Maps

We used the following maps in Level-based Foraging: *Foraging-5x5-2p-1f-v2*, *Foraging-5x5-2p-1f-coop-v2*, *Foraging-5x5-2p-2f-v2*, *Foraging-8x8-2p-2f-coop-v2*, *Foraging-8x8-3p-3f-v2*, *Foraging-10x10-5p-1f-coop-v2*, *Foraging-10x10-3p-5f-v2*, *Foraging-10x10-5p-3f-v2*, *Foraging-10x10-8p-1f-coop-v2*, *Foraging-15x15-8p-1f-coop-v2*

E.2 Selected Hyperparameters

We used the hyperparameters given in Table 4 for all runs of LBF.

| Hyperparameter | Value |
|--|--------------------------------|
| Hidden Dimension | [256] |
| Learning Rate | [5e-4] |
| Network Type | [Fully-connected] |
| Reward Standardisation | [False] |
| Entropy Coefficient | [1e-3] |
| Target network update | [Soft update of 0.01 per step] |
| Number of steps for calculating Return | [10] |
| Number of PERLA samples (K) | [100] |

Table 4: Hyperparameters and optimised values *PERLAISED* variants of IPPO and MAPPO on LBF.

F SMAC Experiments

F.1 Maps

We used the following maps in StarCraft Multiagent Challenge.

Easy - *2m_vs_1z, 2s_vs_1sc, so_many_baneling, bane_vs_bane, 1c3s5z, 2s3z, 3m, 8m, MMM*

Hard - *2c_vs_64zg, 3s5z, 25m*

Very Hard - *3s5z_vs_3s6z, MMM2, corridor*

F.2 Selected Hyperparameters

Hyperparameters used for Multi-agent PPO in the SMAC domain.

| Hyperparameters | value |
|-----------------------------|-------|
| actor lr | 1e-3 |
| critic lr | 5e-4 |
| gamma | 0.99 |
| batch size | 3200 |
| num mini batch | 1 |
| PPO epoch | 10 |
| PPO clip param | 0.2 |
| entropy coef | 0.01 |
| optimiser | ADAM |
| opti eps | 1e-5 |
| max grad norm | 10 |
| actor network | mlp |
| hidden layer | 1 |
| hidden layer dim | 64 |
| activation | ReLU |
| gain | 0.01 |
| eval episodes | 32 |
| use huber loss | True |
| rollout threads | 32 |
| episode length | 100 |
| Number of PERLA samples (K) | 100 |

G Matrix Game Experiments

G.1 Selected Hyperparameters

Hyperparameters used for Multi-agent PPO in the matrix game domain.

| Hyperparameters | value |
|------------------|-------|
| actor lr | 1e-4 |
| gamma | 0.99 |
| batch size | 64 |
| num mini batch | 1 |
| PPO epoch | 5 |
| PPO clip param | 0.2 |
| entropy coef | 0.01 |
| optimiser | ADAM |
| opti eps | 1e-5 |
| max grad norm | 10 |
| actor network | mlp |
| hidden layer | 1 |
| hidden layer dim | 64 |
| activation | ReLU |
| gain | 0.01 |
| eval episodes | 1 |
| use huber loss | False |
| rollout threads | 4 |
| episode length | 1 |

H Multi-agent Mujoco Experiments

Hyperparameters used for Multi-agent PPO in the Multi-Agent MuJoCo domain.

| Hyperparameters | Hopper(3x1) | Swimmer(2x1) | Walker(2x3) |
|------------------|-------------|--------------|-------------|
| actor lr | 5e-4 | 5e-4 | 5e-4 |
| critic lr | 5e-3 | 5e-3 | 5e-3 |
| lr decay | 1 | 1 | 1 |
| γ | 0.99 | 0.99 | 0.99 |
| batch size | 4000 | 4000 | 4000 |
| num mini batch | 40 | 40 | 40 |
| PPO epoch | 5 | 5 | 5 |
| PPO clip param | 0.2 | 0.2 | 0.2 |
| entropy coef | 0.001 | 0.001 | 0.001 |
| optimiser | RMSProp | RMSProp | RMSProp |
| momentum | 0.9 | 0.9 | 0.9 |
| optim eps | 1e-5 | 1e-5 | 1e-5 |
| max grad norm | 0.5 | 0.5 | 0.5 |
| actor network | mlp | mlp | mlp |
| hidden layer | 2 | 2 | 2 |
| hidden layer dim | 128 | 128 | 128 |
| activation | ReLU | ReLU | ReLU |
| eval episodes | 10 | 10 | 10 |
| rollout threads | 4 | 4 | 4 |
| episode length | 1000 | 1000 | 1000 |

I Proofs of Theoretical Results

Proof of Theorem 1

Let us first present a Lemma, which we use to prove the Theorem 1.

Lemma 1. *Given N random variables $(x_i)_{i=1}^N$, where $x_i : \Omega \rightarrow \mathcal{X}_i$ and a measurable function $f : \times_{i=1}^N \mathcal{X}_i \rightarrow \mathbb{R}$, if we define $\tilde{f}(x_1, \dots, x_M) := \mathbb{E}[f(x_1, \dots, x_N) | x_1, \dots, x_M]$ for some $M \leq N$, we have that:*

$$\text{Var}(f(x_1, \dots, x_N)) \geq \text{Var}(\tilde{f}(x_1, \dots, x_M)). \quad (5)$$

Moreover, for a k -sample Monte-Carlo estimator of \tilde{f} given by:

$$\hat{f}(x_1, \dots, x_M) = \frac{1}{k} \sum_{i=1}^k f(x_1, \dots, x_M, x_{M+1}^{(i)}, \dots, x_N^{(i)}),$$

where $x_j^{(i)}$ is the i^{th} sample of x_j we have:

$$\text{Var}(\hat{f}(x_1, \dots, x_M)) = \frac{1}{k} \text{Var}(f(x_1, \dots, x_N)) + \frac{k-1}{k} \text{Var}(\tilde{f}(x_1, \dots, x_M)). \quad (6)$$

Proof. Using the law of total variance we can decompose the variance of \hat{f} as follows:

$$\text{Var}(f(x_1, \dots, x_N)) = \mathbb{E}[\text{Var}(f(x_1, \dots, x_N) | x_1, \dots, x_M)] + \text{Var}(\mathbb{E}[f(x_1, \dots, x_N) | x_1, \dots, x_M])$$

We can now observe that the conditional expectation inside the variance in second term is just \tilde{f} . We therefore get:

$$\text{Var}(f(x_1, \dots, x_N)) = \mathbb{E}[\text{Var}(f(x_1, \dots, x_N) | x_1, \dots, x_M)] + \text{Var}(\tilde{f}(x_1, \dots, x_M)) \quad (7)$$

The first term is an expectation of variance and therefore cannot be negative, this proves the statement in Equation 5. Applying the law of total variance, again, this time for $\hat{f}(x_1, \dots, x_M)$ we get:

$$\text{Var}(\hat{f}(x_1, \dots, x_M)) = \mathbb{E}[\text{Var}(\hat{f}(x_1, \dots, x_M) | x_1, \dots, x_M)] + \text{Var}(\mathbb{E}[\hat{f}(x_1, \dots, x_M) | x_1, \dots, x_M])$$

Note that $\hat{f}(x_1, \dots, x_M)$ is a random variable dependent on (x_{M+1}, \dots, x_N) . Since we estimate \hat{f} by Monte-Carlo method with k samples, we get that the expectation must be equal to the true value \tilde{f} and variance is equal to the variance of samples divided by k . We therefore get:

$$\text{Var}(\hat{f}(x_1, \dots, x_M)) = \frac{1}{k} \mathbb{E}[\text{Var}(f(x_1, \dots, x_M) | x_1, \dots, x_M)] + \text{Var}(\tilde{f}(x_1, \dots, x_N))$$

Substituting an expression for $\mathbb{E}[\text{Var}(f(x_1, \dots, x_M) | x_1, \dots, x_M)]$ from Equation 7, we get:

$$\text{Var}(\hat{f}(x_1, \dots, x_M)) = \frac{1}{k} \text{Var}(f(x_1, \dots, x_N)) + \frac{k-1}{k} \text{Var}(\tilde{f}(x_1, \dots, x_N))$$

which proves the statement in Equation 6. \square

Theorem 1. *The variance of marginalised Q-function \tilde{Q}_i is smaller than that of the non-marginalised Q-function Q_i for any $i \in \mathcal{N}$, that is to say: $\text{Var}(Q_i(s, \mathbf{a})) \geq \text{Var}(\tilde{Q}_i(s, a_i))$. Moreover, for the approximation to the marginalised Q-function (c.f. Equation 2) the following relationship holds:*

$$\text{Var}(\tilde{Q}_i(s, a_i)) = \frac{1}{k} \text{Var}(Q_i(s, \mathbf{a}_{-i}, a_i)) + \frac{k-1}{k} \text{Var}(\tilde{Q}_i(s, a_i)).$$

Proof. Taking the Q-function as f , the action a_i of the i^{th} agent and the state s as random variables x_1, \dots, x_M , and actions of other agents \mathbf{a}_{-i} as remaining variables x_{M+1}, \dots, x_N we immediately obtain the statement of the Theorem from Lemma 1. \square

Proof of Theorem 3

Theorem 3. *Given the same (possibly imperfect) critic, the estimators \mathbf{g}_i^C and \mathbf{g}_i^P have the same expectation, that is:*

$$\mathbb{E}[\mathbf{g}_i^C] = \mathbb{E}[\mathbf{g}_i^P].$$

Proof. Using the tower property of expectation we have:

$$\begin{aligned}
\mathbb{E}[\mathbf{g}_i^C] &= \mathbb{E}\left[\mathbb{E}\left[\sum_{t=0}^{\infty} \gamma^t Q_i(s^t, a_i^t) \nabla_{\theta_i} \log \pi_i(a_i^t | s^t) | a_i^t, s^t\right]\right] \\
&= \mathbb{E}\left[\sum_{t=0}^{\infty} \gamma^t \mathbb{E}[Q_i(s^t, a_i^t) | a_i^t, s^t] \nabla_{\theta_i} \log \pi_i(a_i^t | s^t)\right] \\
&= \mathbb{E}\left[\sum_{t=0}^{\infty} \gamma^t \mathbb{E}[\hat{Q}_i(s^t, a_i^t) | a_i^t, s^t] \nabla_{\theta_i} \log \pi_i(a_i^t | s^t)\right] \\
&= \mathbb{E}\left[\sum_{t=0}^{\infty} \gamma^t \hat{Q}_i(s^t, a_i^t) \nabla_{\theta_i} \log \pi_i(a_i^t | s^t)\right] = \mathbb{E}[\mathbf{g}_i^P],
\end{aligned}$$

where the third equality is due to Monte-Carlo estimates being unbiased. \square

Proof of Theorem 4

Theorem 4. *Given true Q -values, the difference in variances between the decentralised and PERLA estimators admits the following bound:*

$$\text{Var}(\mathbf{g}_i^P) - \text{Var}(\mathbf{g}_i^D) \leq \frac{1}{k} \frac{B_i^2 C^2}{1 - \gamma^2}.$$

Proof. Using the law of total variance on the variance of j -th component of PERLA estimator we get:

$$\text{Var}(g_{i,j}^S) = \mathbb{E}[\text{Var}(g_{i,j}^S | a_i^t, s^t)] + \text{Var}(\mathbb{E}[g_{i,j}^S | a_i^t, s^t])$$

Analogously for the j -th component of the decentralised estimator we get:

$$\text{Var}(g_{i,j}^D) = \mathbb{E}[\text{Var}(g_{i,j}^D | a_i^t, s^t)] + \text{Var}(\mathbb{E}[g_{i,j}^D | a_i^t, s^t])$$

Using the fact that Monte-Carlo estimates are unbiased and that critics are perfect, we get:

$$\text{Var}(\mathbb{E}[g_{i,j}^S | a_i^t, s^t]) = \text{Var}\left(\sum_{t=0}^{\infty} \gamma^t \nabla_{\theta_{i,j}} \log \pi_i(a_t^i | s_t) \mathbb{E}[\hat{Q}(s_t, a_t^i) | a_t^i, s^t]\right) = \text{Var}(\mathbb{E}[g_{i,j}^D | a_i^t, s^t])$$

We therefore obtain:

$$\begin{aligned}
&\text{Var}(g_{i,j}^S) - \text{Var}(g_{i,j}^D) \\
&= \mathbb{E}[\text{Var}(g_{i,j}^S | a_i^t, s^t)] - \mathbb{E}[\text{Var}(g_{i,j}^D | a_i^t, s^t)] \\
&= \mathbb{E}\left[\sum_{t=0}^{\infty} \gamma^{2t} (\nabla_{\theta_{i,j}} \log \pi_i(a_t^i | s_t))^2 (\text{Var}(\hat{Q}(s^t, a_i^t) | a_i^t, s^t) - \text{Var}(\tilde{Q}(s^t, a_i^t) | a_i^t, s^t))\right].
\end{aligned}$$

Since $\tilde{Q}_i(s^t, a_i^t)$ is a deterministic function given a_i^t and s_t , the expression above simplifies to:

$$\text{Var}(g_{i,j}^S) - \text{Var}(g_{i,j}^D) = \mathbb{E}\left[\sum_{t=0}^{\infty} \gamma^{2t} (\nabla_{\theta_{i,j}} \log \pi_i(a_t^i | s_t))^2 \text{Var}(\hat{Q}(s^t, a_i^t) | a_i^t, s^t)\right]$$

Since \hat{Q}_i is a Monte-Carlo approximation of \tilde{Q}_i with k samples of Q_i we get:

$$\text{Var}(g_{i,j}^S) - \text{Var}(g_{i,j}^D) = \mathbb{E}\left[\sum_{t=0}^{\infty} \gamma^{2t} (\nabla_{\theta_{i,j}} \log \pi_i(a_t^i | s_t))^2 \frac{1}{k} \text{Var}(Q(s^t, a^t) | a_i^t, s^t)\right]$$

We can now sum over all components of the gradient vector to obtain:

$$\text{Var}(\mathbf{g}_i^C) - \text{Var}(\mathbf{g}_i^D) = \sum_{j=1}^d \mathbb{E}\left[\sum_{t=0}^{\infty} \gamma^{2t} (\nabla_{\theta_{i,j}} \log \pi_i(a_t^i | s_t))^2 \frac{1}{k} \text{Var}(Q(s^t, a^t) | a_i^t, s^t)\right] \quad (8)$$

$$= \mathbb{E}\left[\sum_{t=0}^{\infty} \gamma^{2t} \|\nabla_{\theta_{i,j}} \log \pi_i(a_t^i | s_t)\|^2 \frac{1}{k} \text{Var}(Q(s^t, a^t) | a_i^t, s^t)\right] \quad (9)$$

$$\leq \frac{B_i^2}{k} \frac{1}{1 - \gamma^2} \mathbb{E}[\text{Var}(Q(s^t, a^t) | a_i^t, s^t)]. \quad (10)$$

We can now upper-bound the variance of the Q-function as follows:

$$\begin{aligned}\text{Var}(Q(s^t, a^t) | a_i^t, s^t) &= \mathbb{E} \left[Q(s^t, a^t)^2 | a_i^t, s^t \right] - \mathbb{E}[Q(s^t, a^t) | a_i^t, s^t]^2 \\ &\leq \mathbb{E} \left[Q(s^t, a^t)^2 | a_i^t, s^t \right] \leq C_i\end{aligned}\quad (11)$$

Combining Equations 9 and 11 completes the proof. \square

Proof of Theorem 5

Theorem 5. *Given true Q-values, the difference in variances between the decentralised and CT-DE estimators admits the following bound:*

$$\text{Var}(\mathbf{g}_i^C) - \text{Var}(\mathbf{g}_i^D) \leq \frac{B_i^2 C^2}{1 - \gamma^2}.$$

Proof. Similar to the proof of Theorem 4, because we assume perfect critics, we have:

$$\text{Var}(\mathbb{E}[g_{i,j}^C | a_i^t, s^t]) = \text{Var} \left(\sum_{t=0}^{\infty} \gamma^t \nabla_{\theta_{i,j}} \log \pi_i(a_t^i | s_t) \mathbb{E}[Q(s_t, a_t^i) | a_i^t, s^t] \right) = \text{Var}(\mathbb{E}[g_{i,j}^D | a_i^t, s^t])$$

We can therefore follow the proof of Theorem 4, using the law of total variance to obtain that:

$$\begin{aligned}\text{Var}(\mathbf{g}_i^C) - \text{Var}(\mathbf{g}_i^D) &\leq \mathbb{E} \left[\sum_{t=0}^{\infty} \gamma^{2t} \|\nabla_{\theta_{i,j}} \log \pi_i(a_t^i | s_t)\|^2 \text{Var}(Q(s^t, a^t) | a_i^t, s^t) \right] \\ &\leq B_i^2 \frac{1}{1 - \gamma^2} \mathbb{E}[\text{Var}(Q(s^t, a^t) | a_i^t, s^t)]\end{aligned}$$

We can now bound the variance of Q-function using the inequality in Equation 11, which completes the proof. \square

Proof of Theorem 6

Theorem 6. *Under the standard assumptions of stochastic approximation theory (Konda and Tsitsiklis 1999), an Actor-Critic algorithm using \mathbf{g}_i^P or \mathbf{g}_i^C as a policy gradient estimator, converges to a local optimum with probability 1, i.e.*

$$P \left(\lim_{k \rightarrow \infty} \|\nabla_{\theta_i} \mathcal{J}(\boldsymbol{\theta}^k)\| = 0 \right) = 1,$$

where $\boldsymbol{\theta}^k$ is the value of vector $\boldsymbol{\theta}$ obtained after the k th update following the policy gradient.

Proof. We prove the convergence by showing that a multi-agent Actor-Critic algorithm based on \mathbf{g}_i^P or \mathbf{g}_i^C can be expressed as a special case of a single agent Actor-Critic algorithm. The convergence of single agent Actor-Critic algorithm has been established by (Konda and Tsitsiklis 1999). First, let us define a joint gradient as a vector consisting of concatenated gradient vectors for each agent. We call them $\mathbf{g}^C = ((\mathbf{g}_1^C)^T, \dots, (\mathbf{g}_N^C)^T)^T$ and $\mathbf{g}^S = ((\mathbf{g}_1^S)^T, \dots, (\mathbf{g}_N^S)^T)^T$ for the centralised and PERLA estimator respectively (we denote the number of agents by N). Let us also define the joint policy for all agents as $\pi(\mathbf{a}|s) = \prod_{i=1}^N \pi_i(a_i|s)$. Since only the policy of the i th agent depends on set of parameters $\boldsymbol{\theta}_i$, we have that:

$$\nabla_{\boldsymbol{\theta}_i} \log \pi(\mathbf{a}|s) = \nabla_{\boldsymbol{\theta}_i} \log \prod_{i=1}^N \pi_i(a_i|s) = \nabla_{\boldsymbol{\theta}_i} \sum_{i=1}^N \log \pi_i(a_i|s) = \nabla_{\boldsymbol{\theta}_i} \log \pi_i(a_i|s)$$

We can therefore write:

$$\nabla_{\boldsymbol{\theta}} \log \pi(\mathbf{a}|s) = ((\nabla_{\boldsymbol{\theta}_1} \log \pi_1(a_1|s))^T, \dots, (\nabla_{\boldsymbol{\theta}_N} \log \pi_N(a_N|s))^T)^T$$

This enables us to express the centralised estimator as:

$$\mathbf{g}^C = \sum_{t=0}^{\infty} \gamma^t Q(s^t, \mathbf{a}^t) \nabla_{\boldsymbol{\theta}} \log \pi(\mathbf{a}^t | s^t)$$

Let us now define a single agent using policy $\pi(\mathbf{a}^t | s^t)$ and taking a multidimensional action \mathbf{a}^t at each step. In such a case, \mathbf{g}^C is an unbiased policy gradient estimate for that agent, which proves the convergence for an Actor-Critic algorithm using \mathbf{g}^C . We have already established in Theorem 3 that $\mathbb{E}[\mathbf{g}_i^C] = \mathbb{E}[\mathbf{g}_i^S]$, which means $\mathbb{E}[\mathbf{g}^C] = \mathbb{E}[\mathbf{g}^S]$. Therefore \mathbf{g}^S is also an unbiased estimate of this special case of single-agent Actor-Critic, which proves its convergence by the same argument. \square